Weak Lensing Peak statistics

Zuhui Fan
Dept. of Astronomy, Peking University

北京大學
PEKING UNIVERSITY

Oct. 17, 2012@NAOC

Outline:

- Introduction
- Weak lensing peak statistics and effects of galaxy intrinsic ellipticities
- Probing cosmology with WL peak statistics
- Discussion

Introduction

More gravity to hold matter together

Repulsive force to accelerate the expansion of the Universe

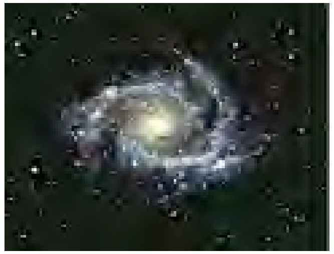

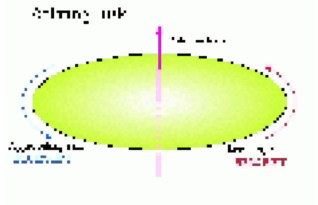

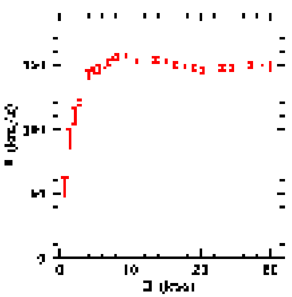

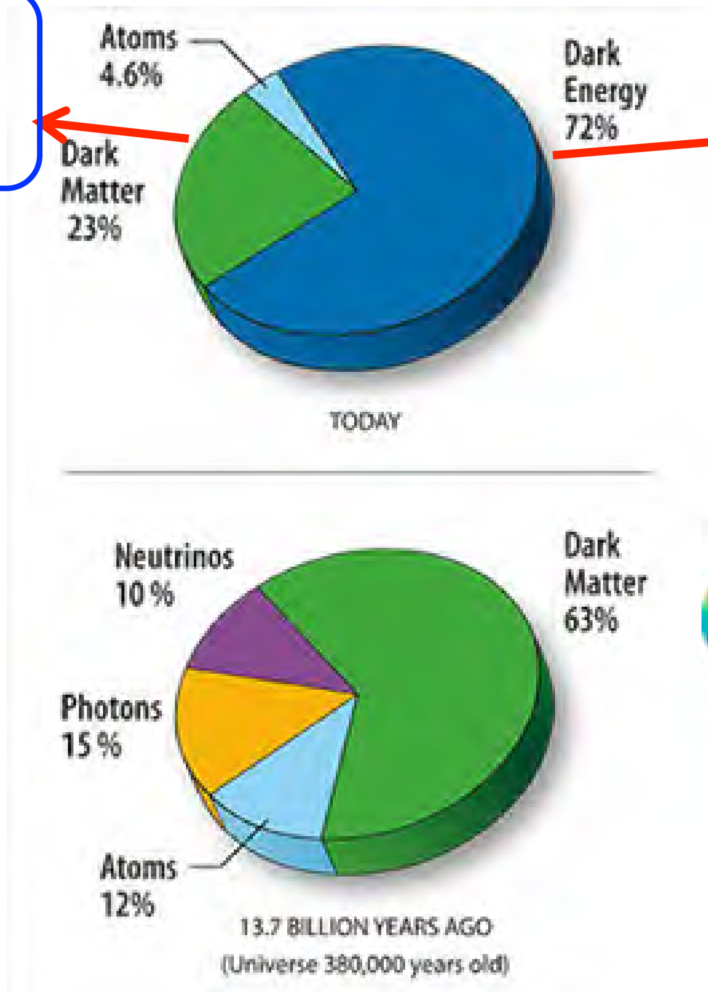

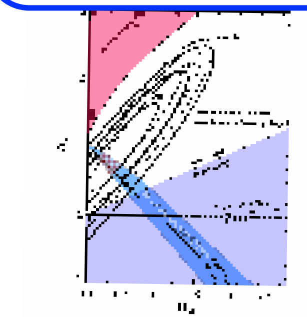

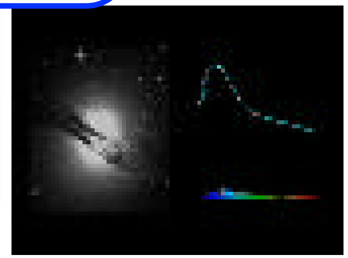

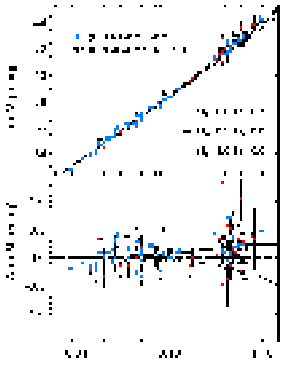

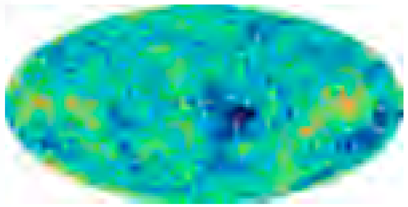

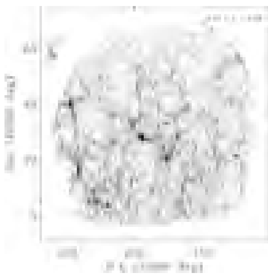

Structures form hierarchically (CDM dominant)

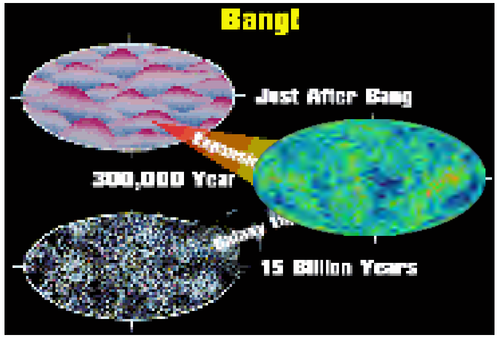

Primordial fluctuations from inflationary epoch $p(k) \sim k^n$

matter composition/ expansion laws

Linear perturbations

Scale-dependence: $T(k)$
$p(k) \sim k^n T(k,t)^2$

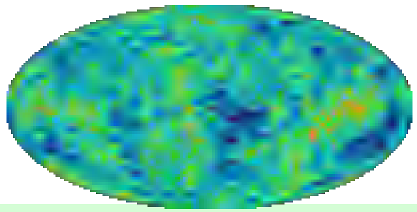

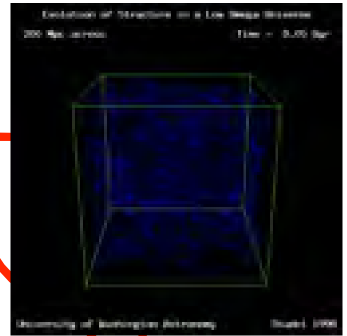

Amplitude growth: $D(t)$
$p(k) = D(t)^2 k^n T(k,t)^2$

nonlinear evolutions
$\delta\rho/\rho > 1$

Gravity plays the dominant role to lay out the skeleton of LSS (dark matter; dark matter halos)

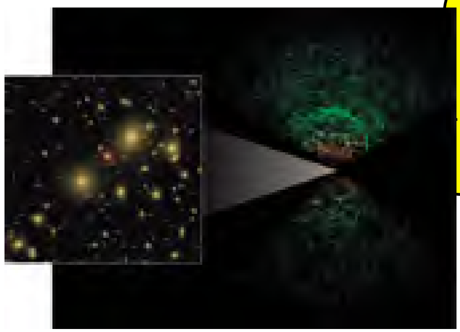

Gas physics
heating, cooling,
star formation/evolution

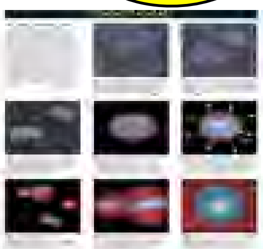

Understanding the nature of dark matter and dark energy has been one of the major efforts in cosmological studies

Weak lensing effect arising from the light deflection by large-scale structures in the universe is among the most important cosmological probes

- "see" dark matter directly
  → powerful probe of the distribution of dark matter
- sensitive to the formation of large-scale structures **AND** the global geometry of the universe
  → highly promising in dark energy studies

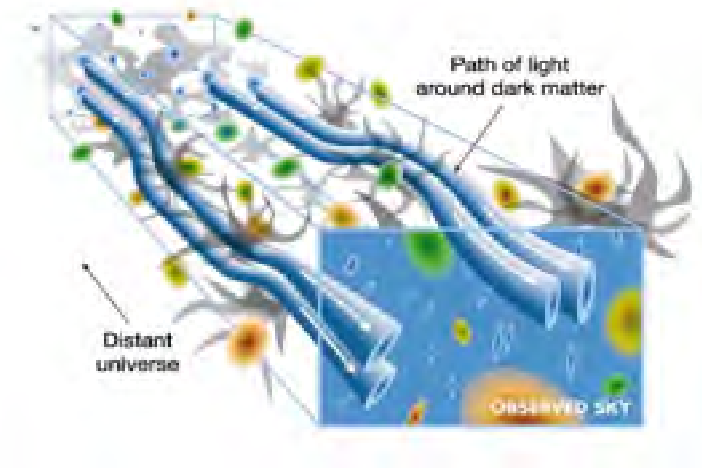

Wittman et al. 2000, Nature

Weak lensing effects: commonly exist in the universe

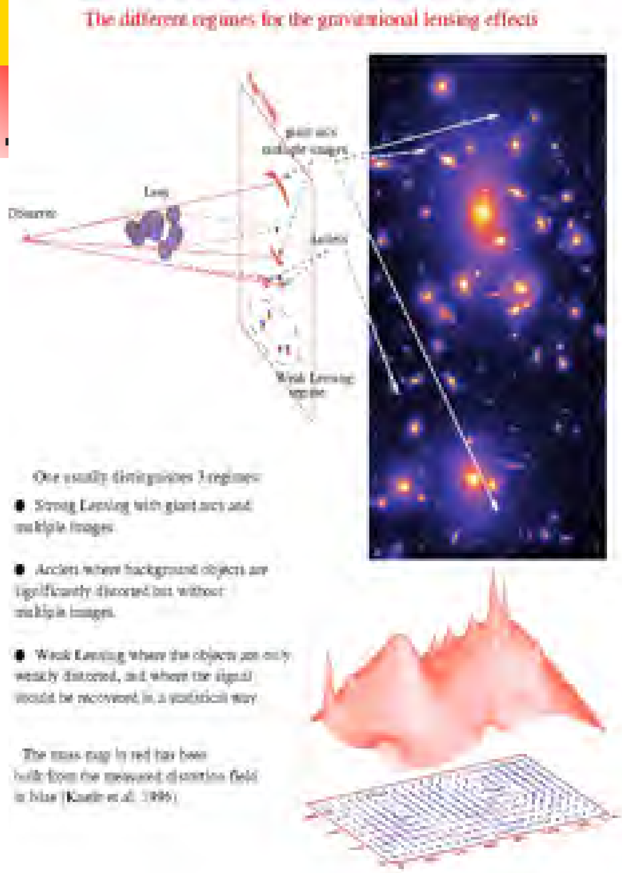

weak image distortions/flux changes

occur outside the cluster central
region and extends to large radii
→ powerful probe to study the overall
mass distribution of clusters and even beyond

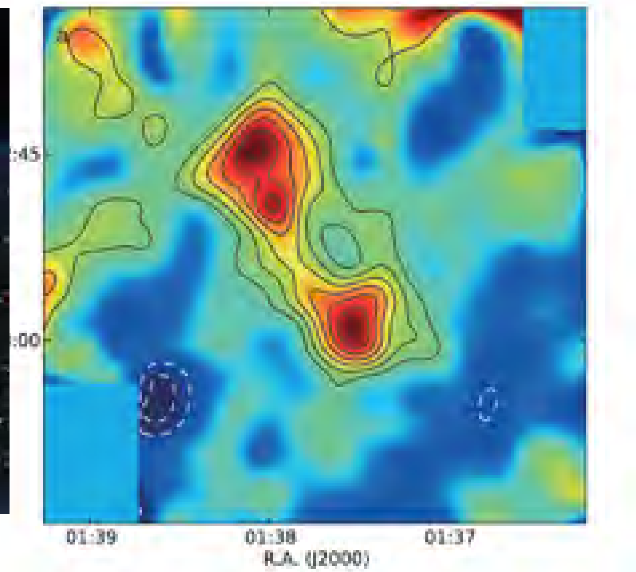

Dietrich et al. 2012, Nature, 487,202

Weak lensing effects: commonly exist in the universe

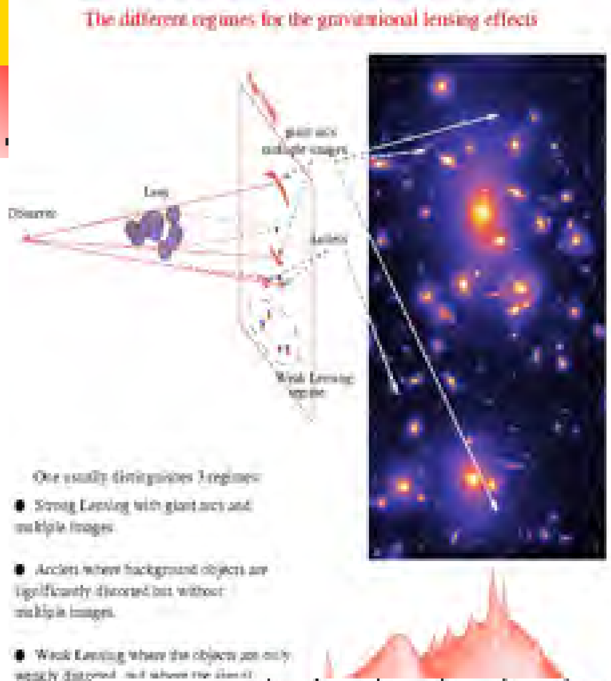

weak image distortions/flux changes

occur outside the cluster central region and extends to large radii
→ powerful probe to study the overall mass distribution of clusters and even beyond

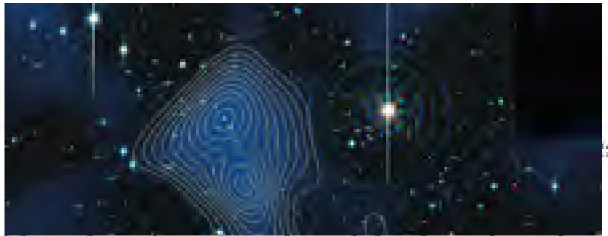

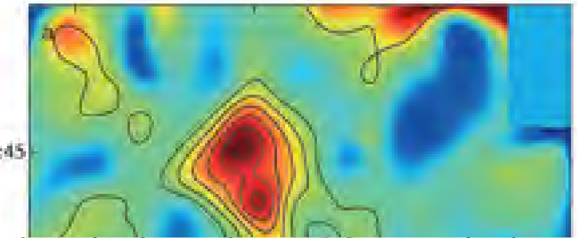

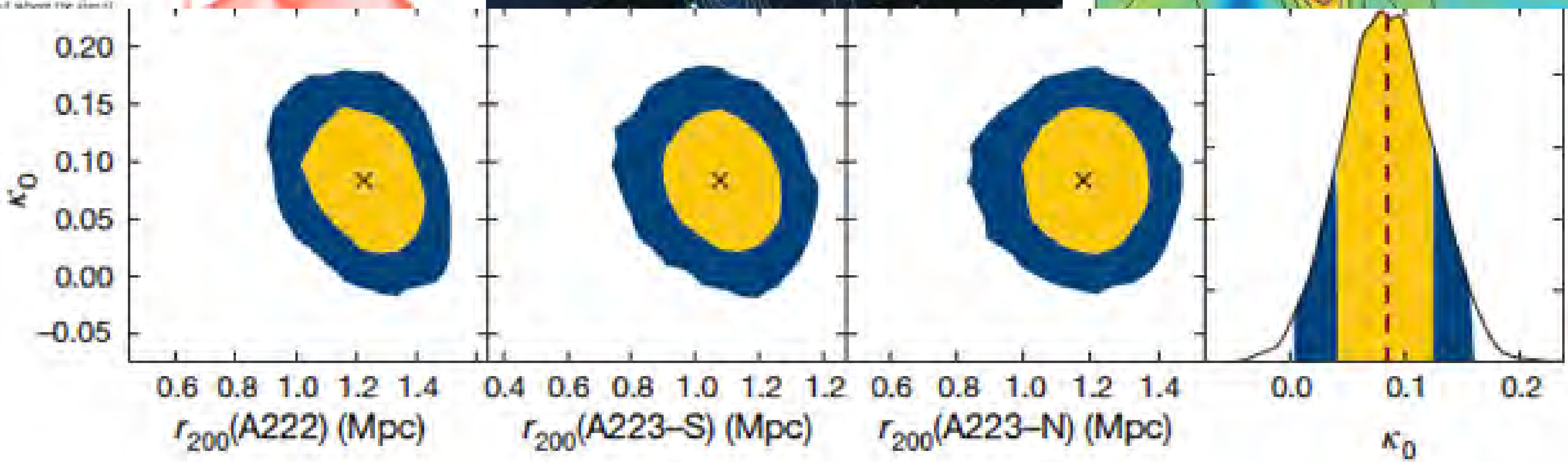

Gravity induced

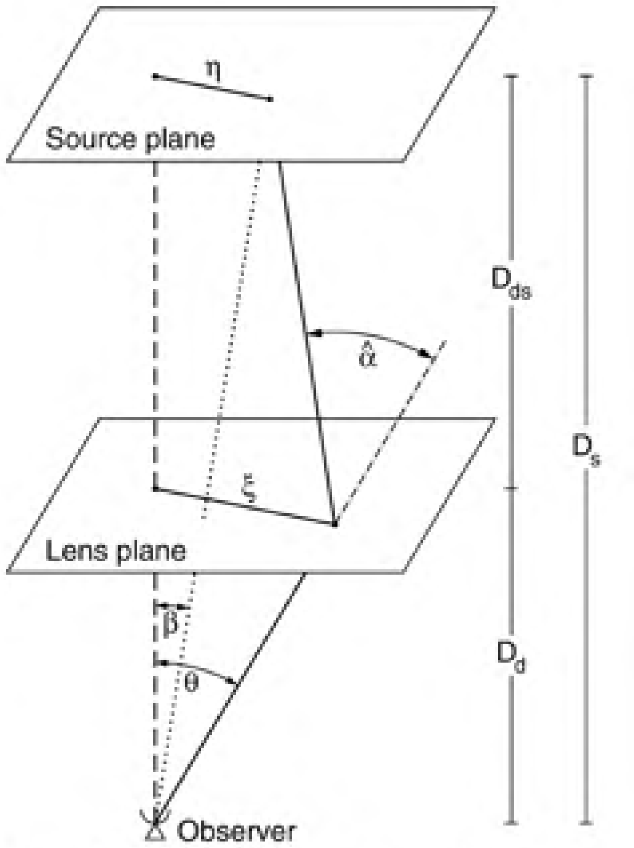

Fig. 11. Sketch of a typical gravitational lens system.

For a single lens

$$\Sigma(\xi) \equiv \int \mathrm{d}r_3\, \rho(\xi_1, \xi_2, r_3)$$

deflection angle

$$\hat{\boldsymbol{\alpha}}(\boldsymbol{\xi}) = \frac{4G}{c^2} \int \mathrm{d}^2\xi'\, \Sigma(\boldsymbol{\xi}') \frac{\boldsymbol{\xi} - \boldsymbol{\xi}'}{|\boldsymbol{\xi} - \boldsymbol{\xi}'|^2}$$

lensing equation

$$\boldsymbol{\eta} = \frac{D_s}{D_d} \boldsymbol{\xi} - D_{ds} \hat{\boldsymbol{\alpha}}(\boldsymbol{\xi})$$

$$\boldsymbol{\beta} = \boldsymbol{\theta} - \frac{D_{ds}}{D_s} \hat{\boldsymbol{\alpha}}(D_d \boldsymbol{\theta}) \equiv \boldsymbol{\theta} - \boldsymbol{\alpha}(\boldsymbol{\theta}) \qquad \boldsymbol{\alpha} = \nabla\psi$$

The observational effects can be described by a mapping between θ and β through surface brightness conservation

$$I(\boldsymbol{\theta}) = I^{(s)}[\boldsymbol{\beta}(\boldsymbol{\theta})]$$

small source

$$I(\boldsymbol{\theta}) = I^{(s)}[\boldsymbol{\beta}_0 + \mathscr{A}(\boldsymbol{\theta}_0) \cdot (\boldsymbol{\theta} - \boldsymbol{\theta}_0)]$$

$$\mathscr{A}(\boldsymbol{\theta}) = \frac{\partial \boldsymbol{\beta}}{\partial \boldsymbol{\theta}} = \left(\delta_{ij} - \frac{\partial^2 \psi(\boldsymbol{\theta})}{\partial\theta_i \partial\theta_j}\right) = \begin{pmatrix} 1 - \kappa - \gamma_1 & -\gamma_2 \\ -\gamma_2 & 1 - \kappa + \gamma_1 \end{pmatrix}$$

Bartelmann & Schneider 2001, Phys. Report

convergence $\nabla^2\psi(\theta) = 2\kappa(\theta)$ $\kappa(\theta) = \dfrac{\Sigma(D_d\theta)}{\Sigma_{cr}}$ $\Sigma_{cr} = \dfrac{c^2}{4\pi G}\dfrac{D_s}{D_d D_{ds}}$

shear $\gamma \equiv \gamma_1 + i\gamma_2 = |\gamma| e^{2i\varphi}, \quad \gamma_1 = \frac{1}{2}(\psi_{,11} - \psi_{,22}), \quad \gamma_2 = \psi_{,12}$

magnification
$$\mu(\vec{\theta}_0) = \frac{\int I(\vec{\theta})d\vec{\theta}}{\int I^{(s)}(\vec{\beta})d\vec{\beta}} \approx \frac{\int I^{(s)}[\vec{\beta}_0 + A(\vec{\theta}_0)\bullet(\vec{\theta} - \vec{\theta}_0)]d\vec{\theta}}{\int I^{(s)}(\vec{\beta})d\vec{\beta}}$$
$$= \frac{1}{\det(A)} = \frac{1}{(1-\kappa)^2 - (\gamma_1^2 + \gamma_2^2)} = \frac{1}{(1-\kappa)^2 - |\gamma|^2}$$

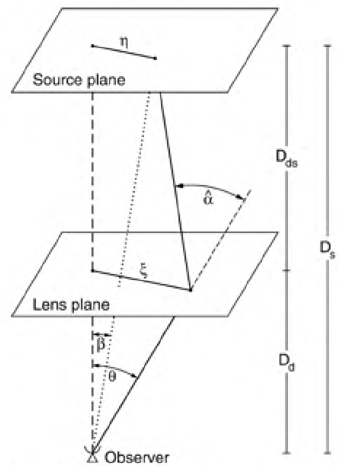

Fig. 11. Sketch of a typical gravitational lens system.

shear distortion: axial ratio of ellipse $\dfrac{1-\kappa-|\gamma|}{1-\kappa+|\gamma|}$

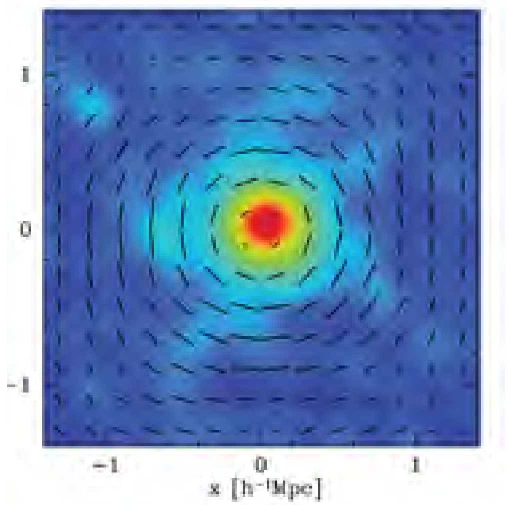

lensing

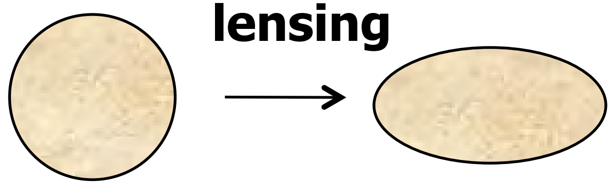

circular source **ellipses**

Cosmic shear: cumulative effects of intervening deflections between a source and an observer

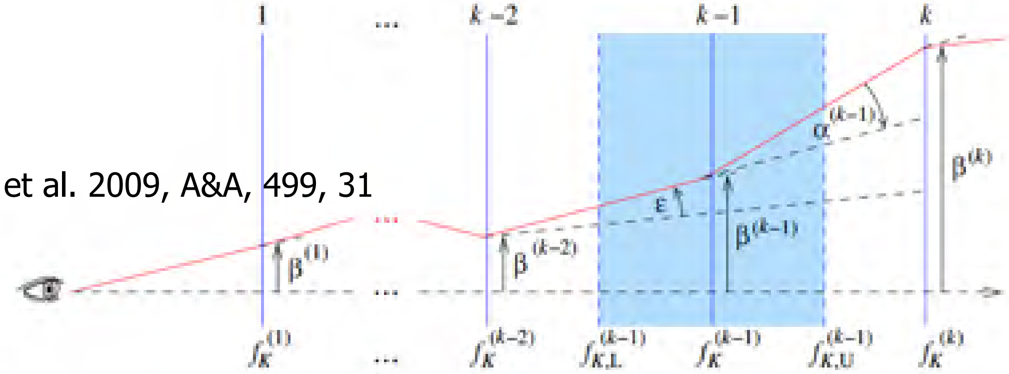

Hilbert et al. 2009, A&A, 499, 31

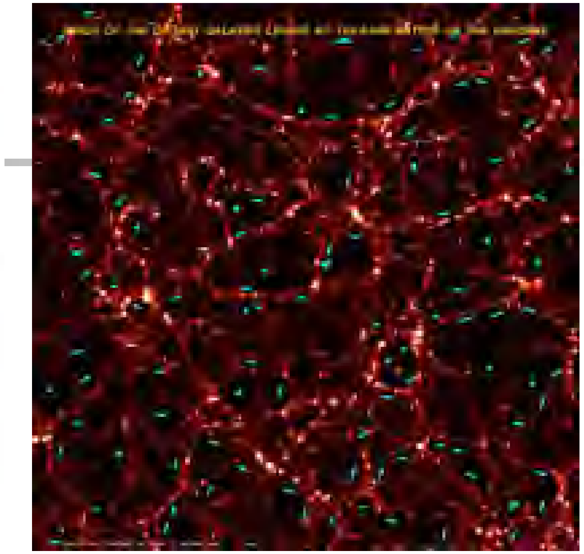

For weak cosmic shear, Born approximation can be applied which calculates the light deflection along the unperturbed light ray.

$$\boldsymbol{\alpha}(\boldsymbol{\theta}, w) = \frac{f_K(w)\boldsymbol{\theta} - \boldsymbol{x}(\boldsymbol{\theta}, w)}{f_K(w)} = \frac{2}{c^2}\int_0^w \mathrm{d}w' \frac{f_K(w - w')}{f_K(w)} \nabla_\perp \Phi[f_K(w')\boldsymbol{\theta}, w']$$

$$\kappa_{\rm eff}(\boldsymbol{\theta}, w) = \frac{1}{2}\nabla_{\boldsymbol{\theta}} \cdot \boldsymbol{\alpha}(\boldsymbol{\theta}, w)$$

$$= \frac{1}{c^2}\int_0^w \mathrm{d}w' \frac{f_K(w - w') f_K(w')}{f_K(w)} \frac{\partial^2}{\partial x_i \partial x_i} \Phi[f_K(w')\boldsymbol{\theta}, w']$$

$$\mathcal{A}(\boldsymbol{\theta}, w) = I - \frac{\partial \boldsymbol{\alpha}(\boldsymbol{\theta}, w)}{\partial \boldsymbol{\theta}} = \frac{1}{f_K(w)} \frac{\partial \boldsymbol{x}(\boldsymbol{\theta}, w)}{\partial \boldsymbol{\theta}}$$

Weak lensing studies are challenging

* galaxies are not intrinsically round

→ intrinsic ellipticities can be much larger than weak lensing effects

→ **large number of background faint galaxies are needed**

* accurate measurements of light distribution of far-away galaxies

sub-arcsecond seeing conditions

* atmospheric disturbance PSF

* telescope PSF

(Great10, Great08, STEP)

* accurate calibration of the redshift distribution of source galaxies (PATH program)

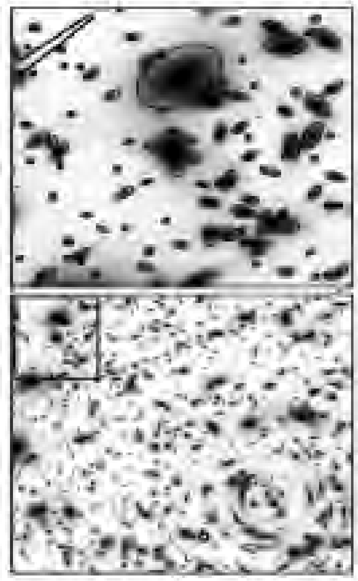

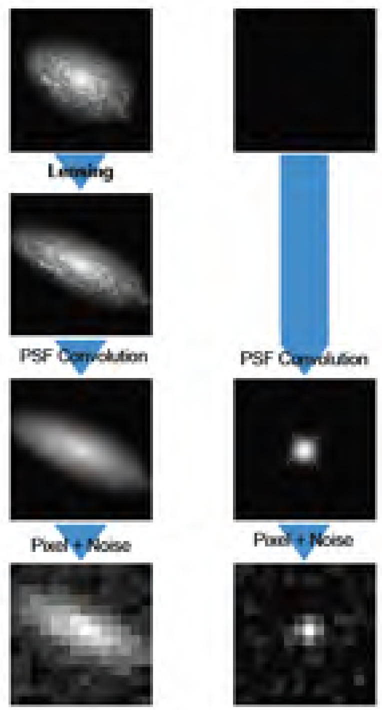

A. Amara 2011,arXiv: 1109.3410

Observational + theoretical + statistical methodology developments → weak lensing analyses are becoming feasible

Cosmic shear correlation analyses

With redshift information of of background galaxies, tomographic cosmic shear correlation analyses are expected to contribute importantly to future cosmological studies

** Two-point correlation analyses contain only part of the information, especially considering nonlinear structure formation

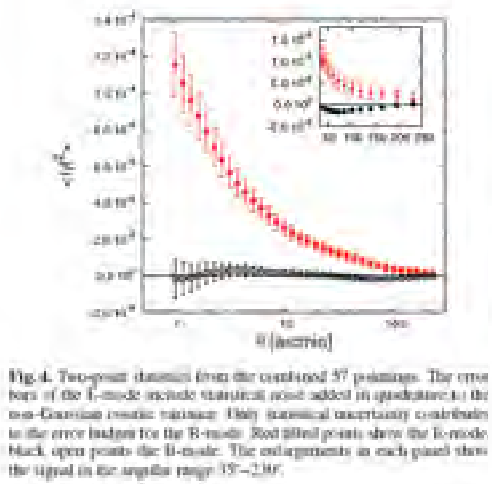

Fu et al. 2008 A&A (CFHTLS, 57 sq. deg)

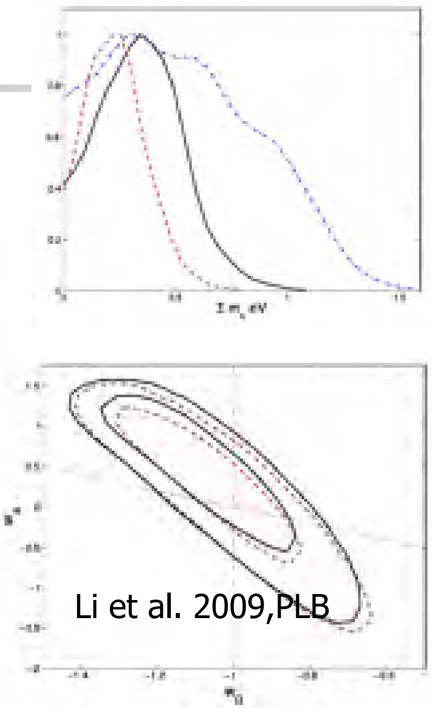

Li et al. 2009,PLB

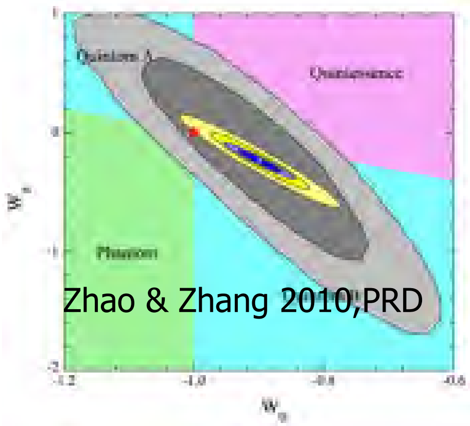

Zhao & Zhang 2010,PRD

Weak lensing peak statistics

Nonlinear structures, such as massive clusters, are expected to generate high lensing signals, and can appear as peaks in weak-lensing reconstructed maps.

→ *Peak statistics can provide important complementary information in weak lensing cosmological studies*

Selection function is insensitive to baryonic physics

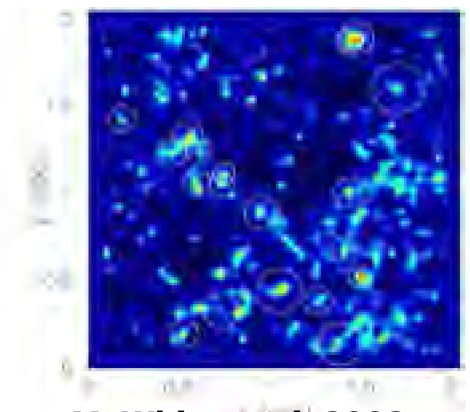

M. White et al. 2002
T. Hamana et al. 2004
Tang & Fan 2005

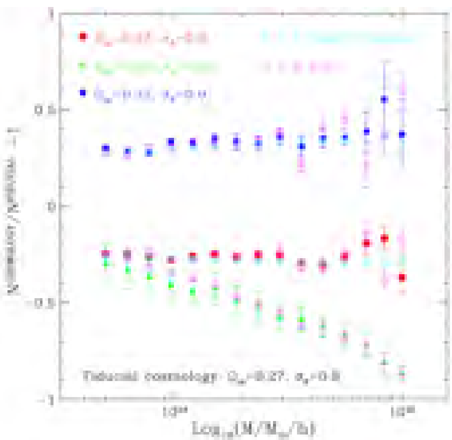

L. Marian et al. 2009

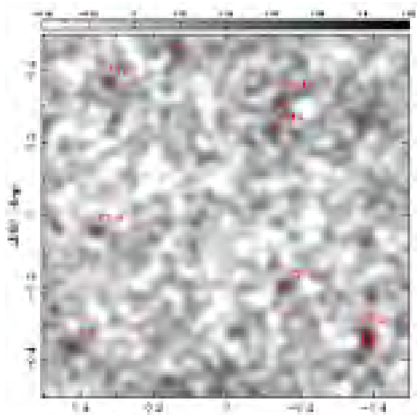

Gavazzi & Soucail 2006
CFHTLS Deep

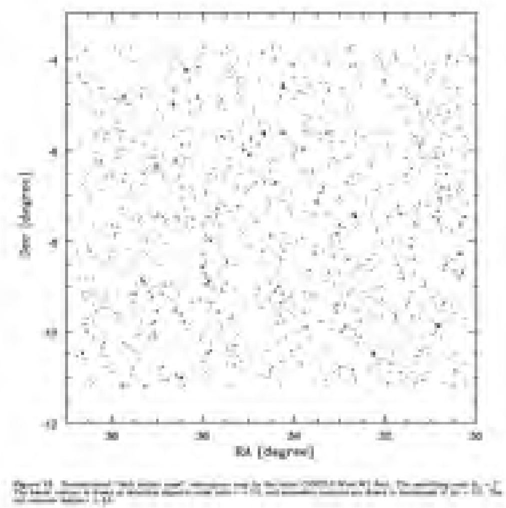

Shan et al. 2012, CFHTLS

However, different effects can affect weak lensing peak statistics

The correspondence between WL peaks and massive clusters is affected by
* projection effects from large-scale structures along line of sights
* noise from intrinsic ellipticities of background galaxies
* observational effects, such as mask effects from bad/missing data

→ Produce 'false' peaks
→ Affect 'true' peaks from clusters

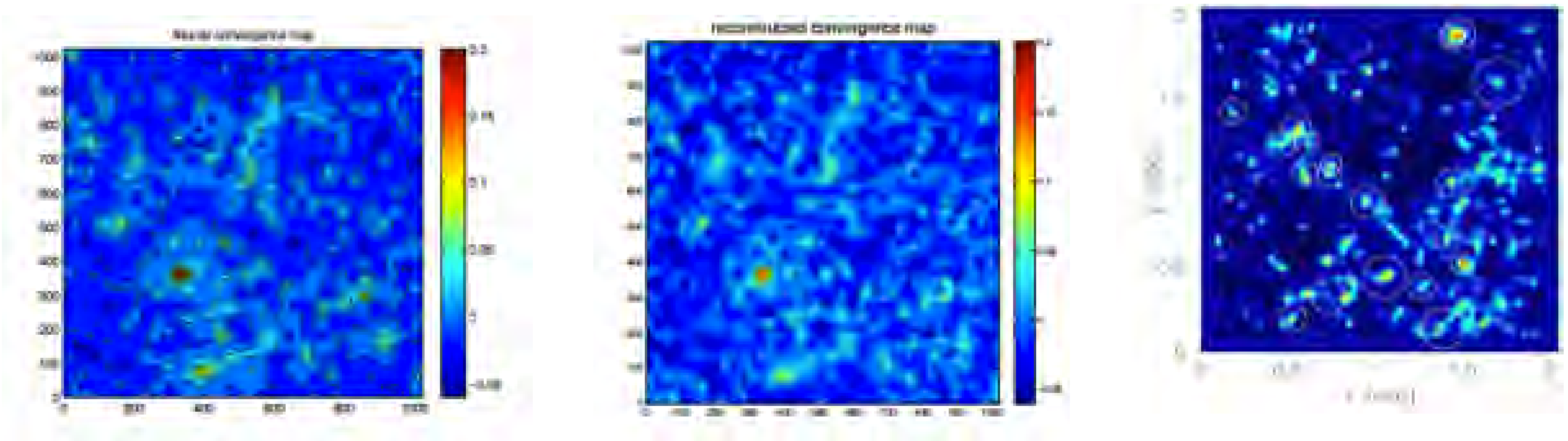

Liu et al. 2012

One way to overcome these problems

Create a large library of mock data from different cosmological models taken into account all the effects

→ compare with observational data

→ constraints on cosmological parameters

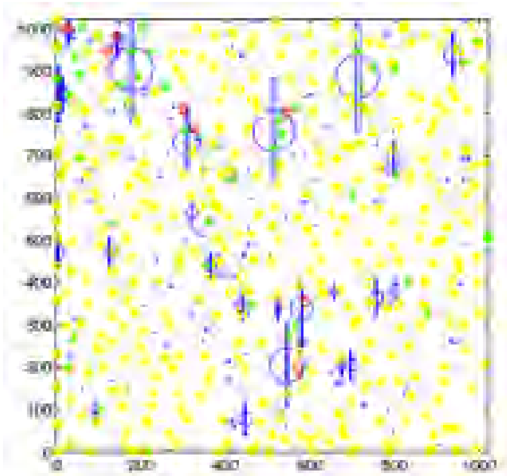

Liu et al. 2012

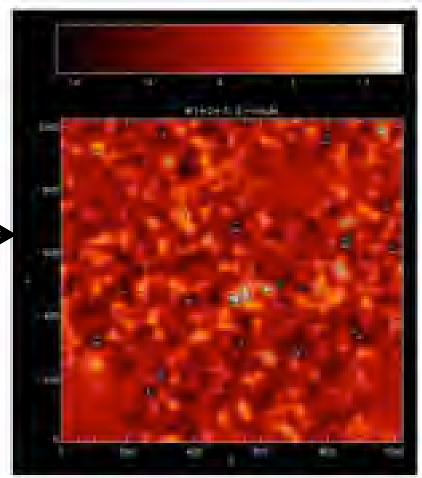

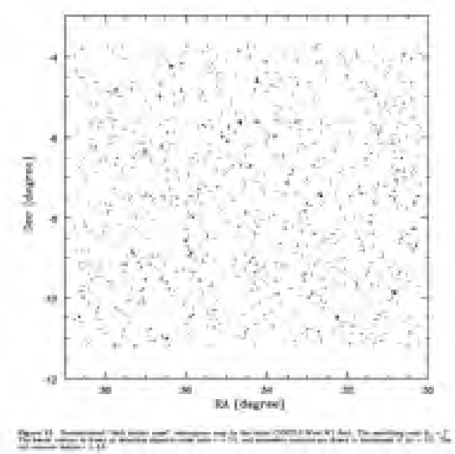

Shan et al. 2012

** Expensive and cover limited parameter space

** Even we can run simulations for a large number of models,
it is still highly desirable to understand different effects physically.

Effects of galaxy intrinsic ellipticities on WL peak statistics (Fan et al. 2010)

In the weak lensing regime,

lensing shear

intrinsic ellipticity

Observed ellipticity $\longleftarrow$ $\varepsilon_\alpha^{(o)} \approx \gamma_\alpha + \varepsilon_\alpha^{(s)}, \quad \alpha = 1,2$

$$\kappa_n(\mathbf{k}) = c_\alpha \varepsilon_\alpha^{(o)} = \kappa(\mathbf{k}) + c_\alpha \varepsilon_\alpha^{(S)},\ c_\alpha = [\cos 2\varphi, \sin 2\varphi] \quad \mathbf{k} \approx k[\cos\varphi, \sin\varphi]$$

Smoothed shear and convergence

$$\Sigma_\alpha^{(O)}(\boldsymbol{\theta}) \approx \Gamma_\alpha(\boldsymbol{\theta}) + \Sigma_\alpha^{(s)}(\boldsymbol{\theta}) = \Gamma_\alpha(\boldsymbol{\theta}) + \frac{1}{n_g}\sum_{i=1}^{N_g} W(\boldsymbol{\theta} - \boldsymbol{\theta}_i)\varepsilon_\alpha^{(s)}(\boldsymbol{\theta}_i), \quad \alpha = 1,2$$

$$\mathrm{K}_N(\boldsymbol{\theta}) = K(\boldsymbol{\theta}) + N(\boldsymbol{\theta}) = \int d\mathbf{k}\, \exp(-i\mathbf{k} \bullet \boldsymbol{\theta}) c_\alpha(\mathbf{k}) \Sigma_\alpha^{(o)}(\mathbf{k})$$

Gaussian noise field

Number of peaks from $K_N(\vec{\theta}) = K(\vec{\theta}) + N(\vec{\theta})$ is ***NOT*** the simple summation of

$$N_{peak}[K(\theta)+N(\theta)] \neq N_{peak}[K(\theta)] + N_{peak}[N(\theta)]$$

The two sides affect each other mutually, and can be analyzed statistically

Halo regions: ** halo peak is affected by noise
** number of noise peaks is enhanced by halo mass distribution

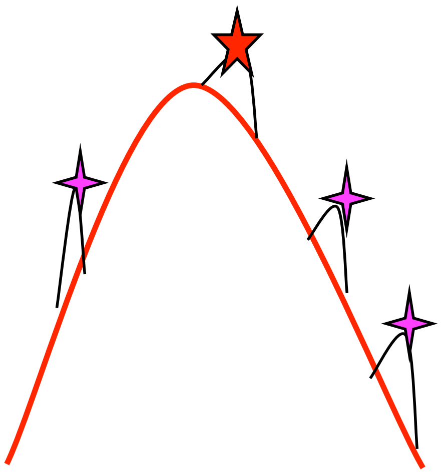

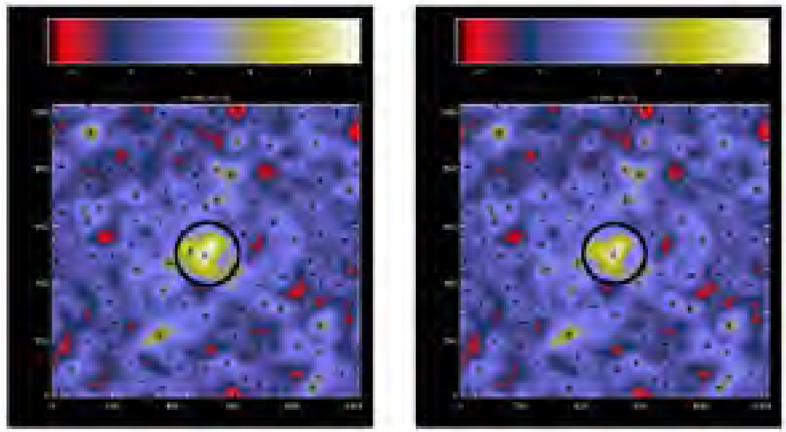

Both the position and the height of the halo peak are affected by noise

Halo peak height: systematically shifted to higher end
→ Noise can enhance peak detections

$$p(\nu) = \frac{n_{peak}(\nu)}{[\int n_{peak}(\nu')d\nu']}$$

K, K^1, K^2, K^{11} and K^{22} at $\tilde{R} = 0$

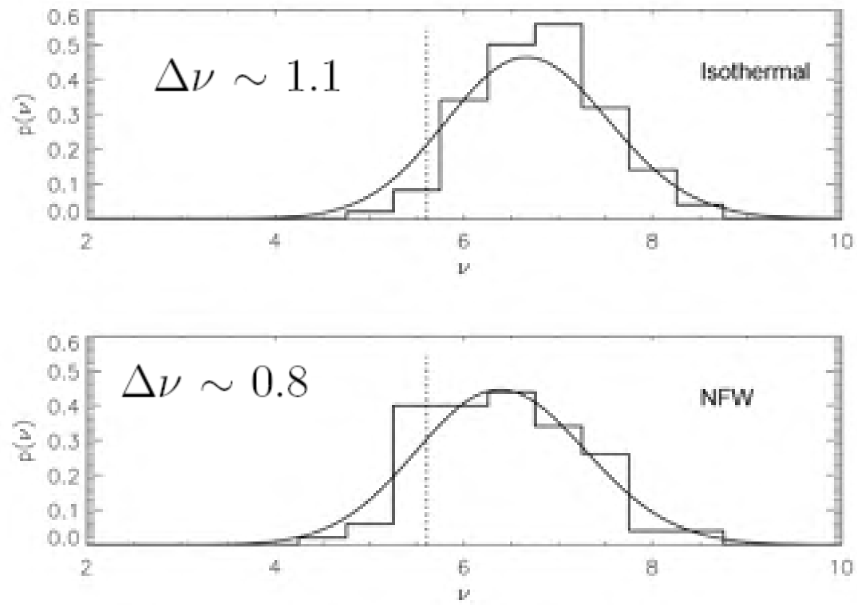

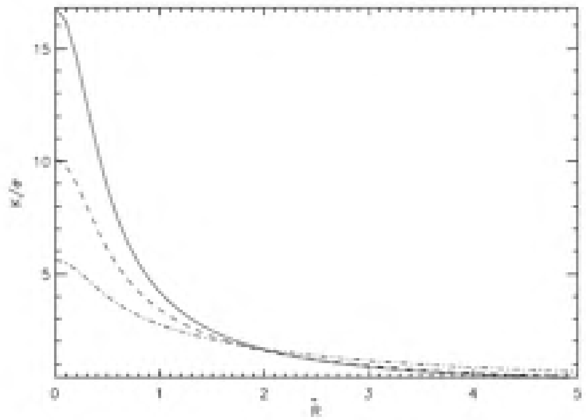

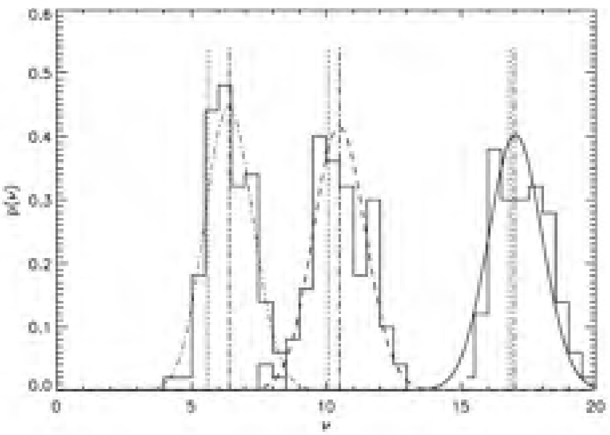

The more centrally concentrated the profile is, the smaller Δv is.

The histogram is for the result from our Monte Carlo simulations. The vertical dotted line indicates the value of $\nu = 5.6$, the true peak height of the considered cluster. The cluster parameters are the same as those in Figure 2.

The systematic shift is closely related to the statistical properties of the Gaussian random field

For a pure Gaussian noise field N without cluster, the peak height distribution is peaked at $\nu_p \approx 1$ for $\gamma \approx 0.7$ rather than $\nu_p = 0$

For a cluster with a rather flat density distribution, the peak height distribution for the total field K+N is peaked at $\sim K_0 + \nu_p$ at the center. In general, K, K^1, K^2, K^{11} and K^{22} at $\tilde{R} = 0$ affect the peak height distribution.

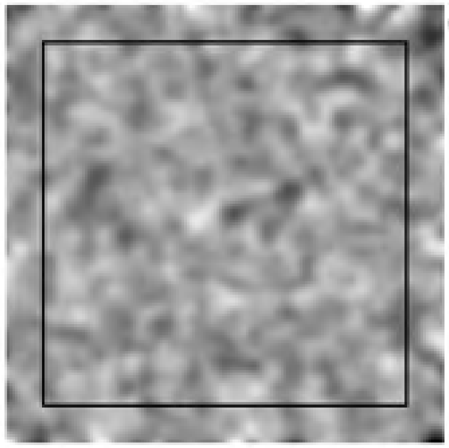

Van Waerbeke 2000

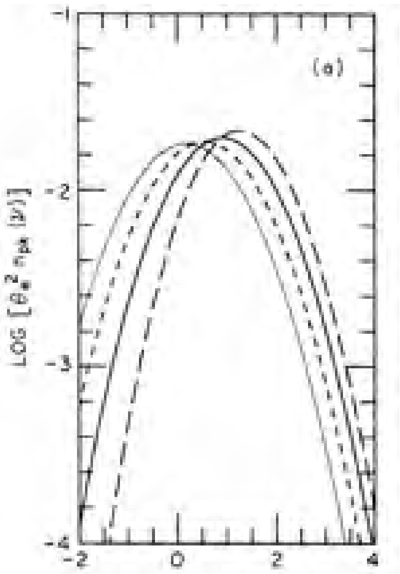

Bond & Efstathiou 1987

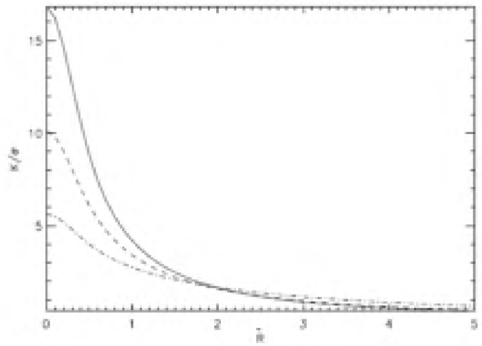

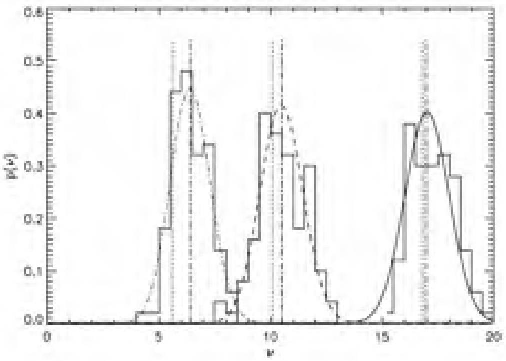

The more centrally concentrated the profile is, the smaller Δv is.

Statistical peak abundances over a large field

Halo region + field region

$$n_{peak}(\nu)d\nu = n^c_{peak}(\nu)d\nu + n^n_{peak}(\nu)d\nu$$

$$n^c_{peak}(\nu) = \int dz \frac{dV(z)}{dz d\Omega} \int dM \boxed{n(M,z)} \boxed{f(\nu, M, z)}$$

$$f(\nu, M, z) = \int_0^{R_{vir}} dR\ (2\pi R)\ n_{peak}(\nu, M, z)$$

$$n^n_{peak}(\nu) = \frac{1}{d\Omega}\left\{n_{ran}(\nu)\left[d\Omega - \int dz \frac{dV(z)}{dz} \int dM\ n(M,z)\ (\pi R^2_{vir})\right]\right\}$$

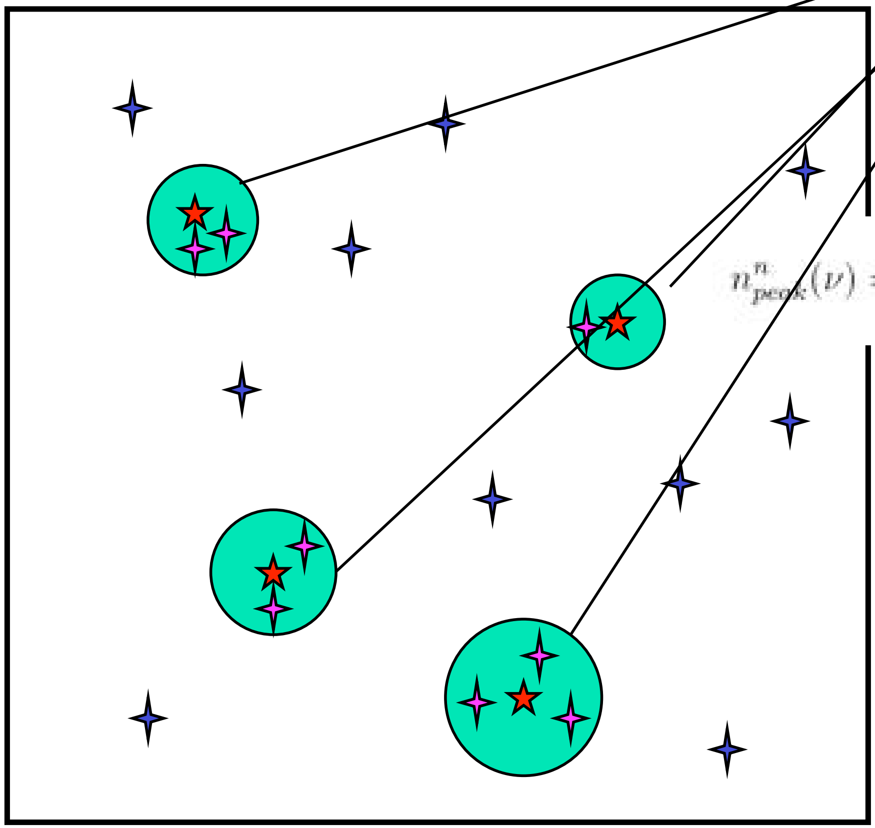

Halo region:

** Halo peak is affected by noise
** Number of noise peaks is enhanced by halo mass distribution

Comparison with simulations
(*http://mwhite.berkeley.edu/Lensing*)

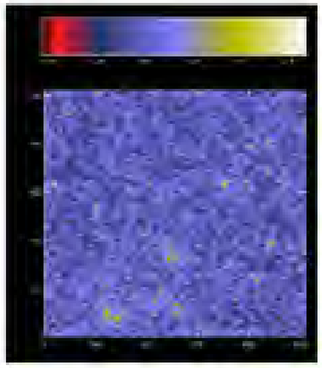

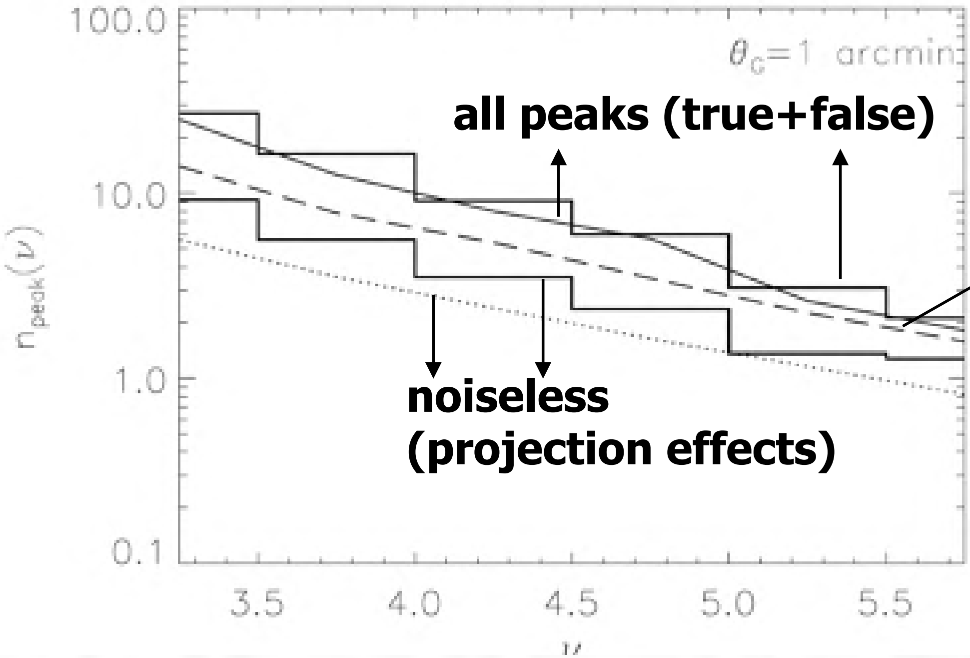

Fig. 10. The differential peak height distribution in 1 deg². The histograms are for the results averaged over 16 ray-tracing simulations with 3 × 3 deg² each by White and Vale (2004). The lower and upper histograms correspond to the results without and with noise included. The dotted line is for ... considering only NFW halos without noise [Eq. (40)]. The long-dash... of dark matter halos including the noise effects on the their peak heights calculated from Eq. (41) and Eq. (31). The solid line is for the prediction from Eq. (35)-Eq. (38) including the full noise effects.

Fan et al. 2010

Effect on halo peak height

$$n_{peak}(\nu) = \int dz \frac{dV(z)}{dz d\Omega} \int dM\, n(M,z)\, p_{peak}(\nu, M, z)$$

$$p(\nu) = \frac{n_{peak}(\nu)}{[\int n_{peak}(\nu')d\nu']}$$

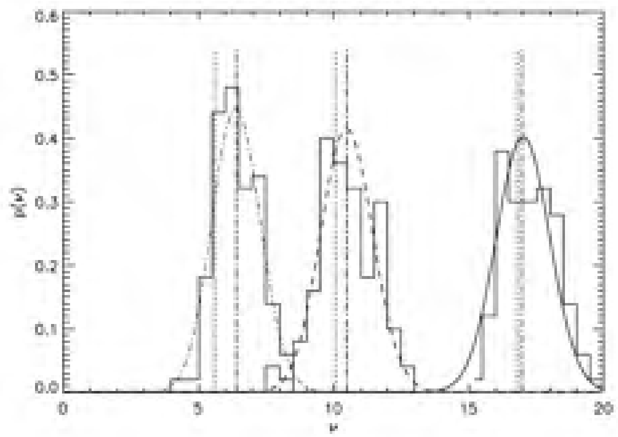

Probing cosmology with WL peak statistics

Our HOD-like model can calculate the total peak abundances:

halo mass function, halo density profile

→ cosmological studies with total number of peaks

** noise peaks near halo regions carry information of the halo density profiles.

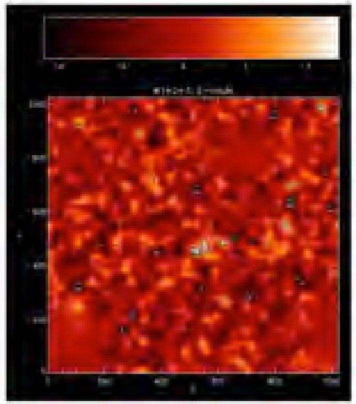

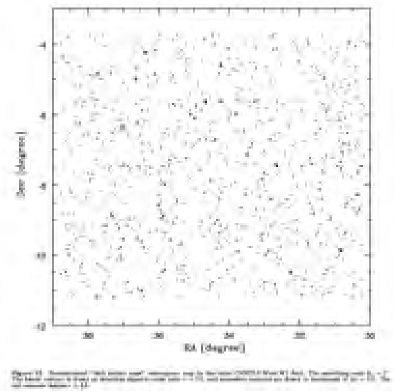

1 arcmin

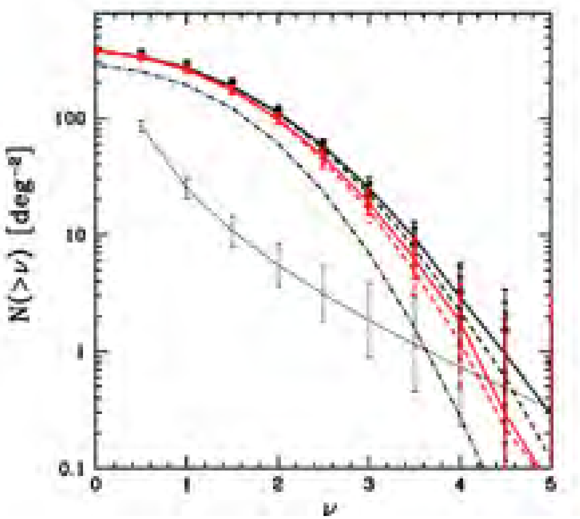

2 arcmin

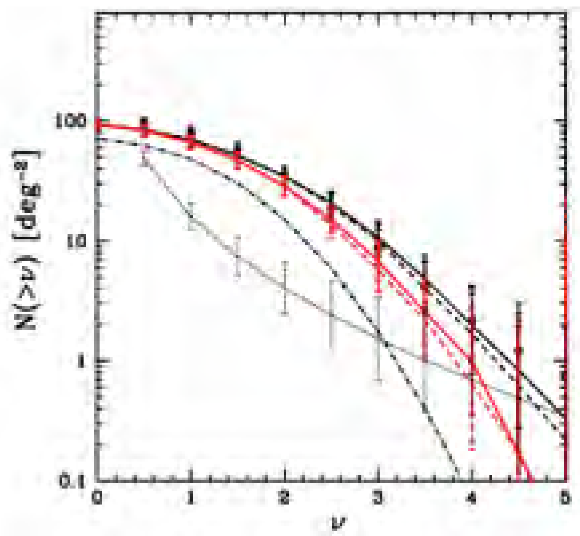

Shan et al. 2012

CFHTLS 72 deg^2 analyses

Cosmological constraints with (total) WL peak statistics

(Liu et al. 2012) → very promising

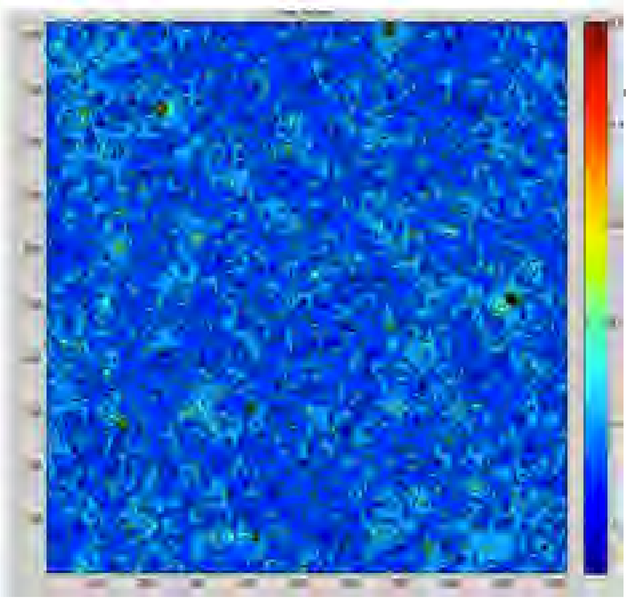

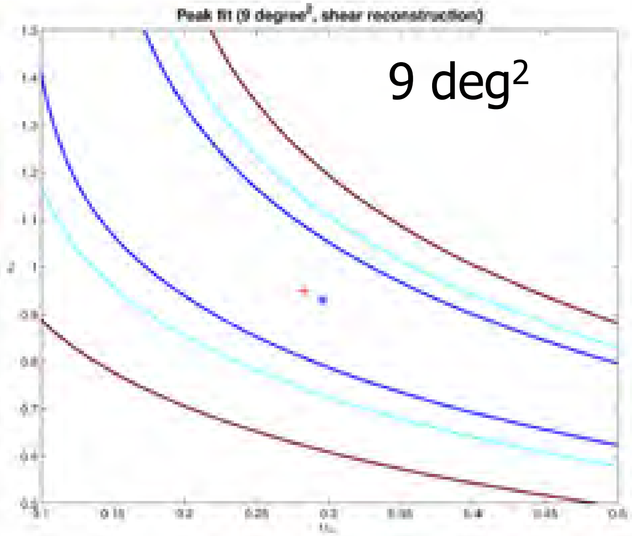

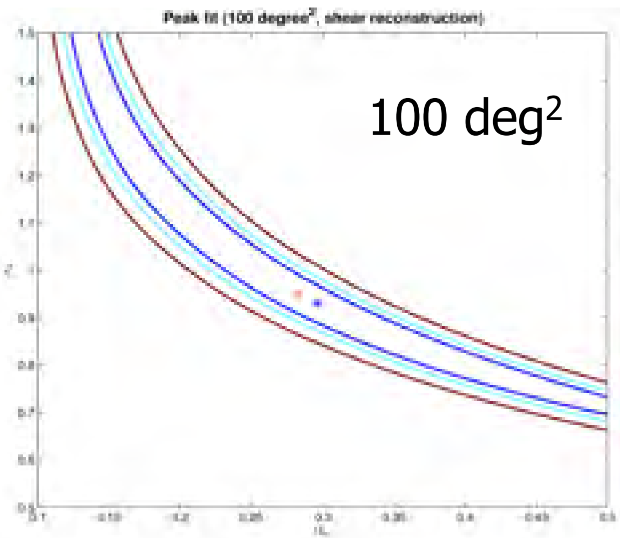

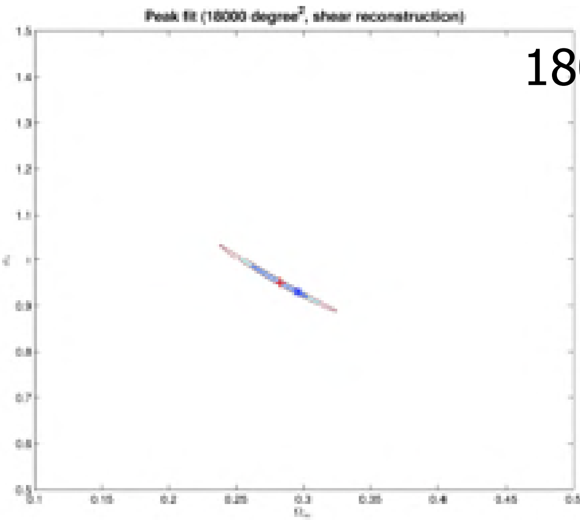

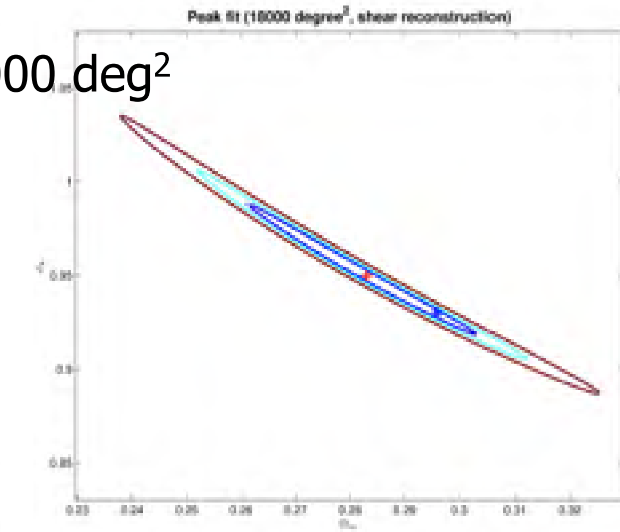

Bias induced by noise from ‘true’ peak statistics

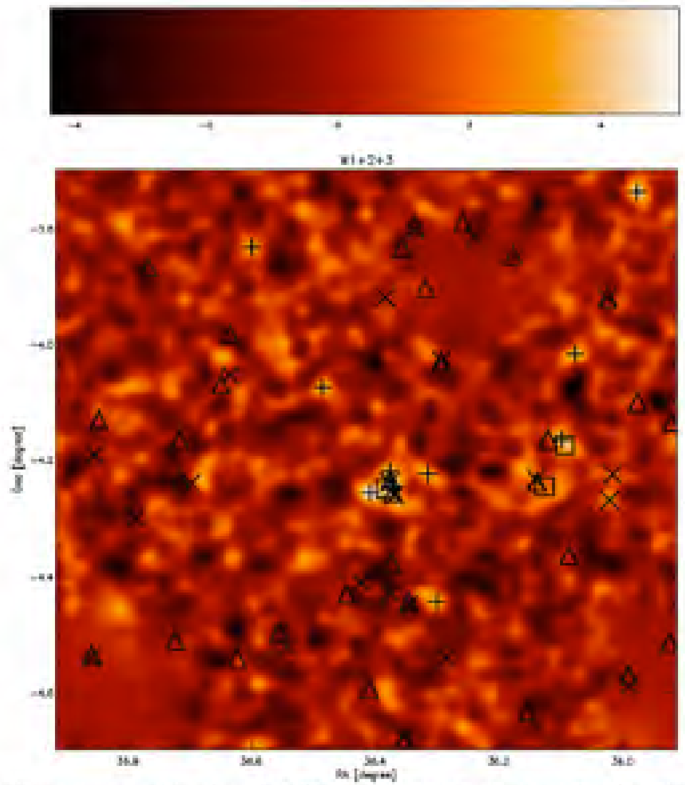

Figure 17. Reconstructed lensing convergence signal to noise map for the W1+2+3 pointing, plus overlays showing optically and X-ray selected cluster counterparts. The smoothing scale of the background map is $\theta_G = 1'$. Symbols indicate the positions of +: lensing peaks detected with $\nu > 3.5$ in the $\theta_G = 1'$ map, □: lensing peaks detected with $\nu > 3.5$ in the $\theta_G = 2'$ map, △: optically detected clusters in the K2 catalog, and ×: X-ray selected clusters found in XMM-LSS (Adami et al. 2011).

‘true’ peak statistics: optical/x ray → find ‘true’ peaks associated with real clusters

Shan et al. 2012

Our analyses show however, even these 'true' peaks are affected by noise. Without suitably taking into account the noise effects, the inferred cosmological parameters can be largely biased.

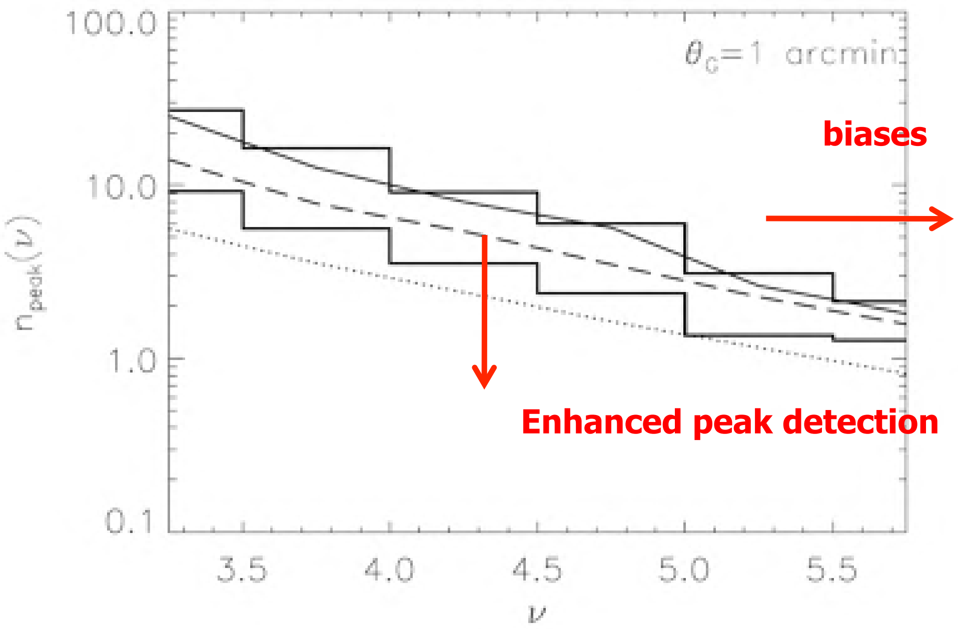

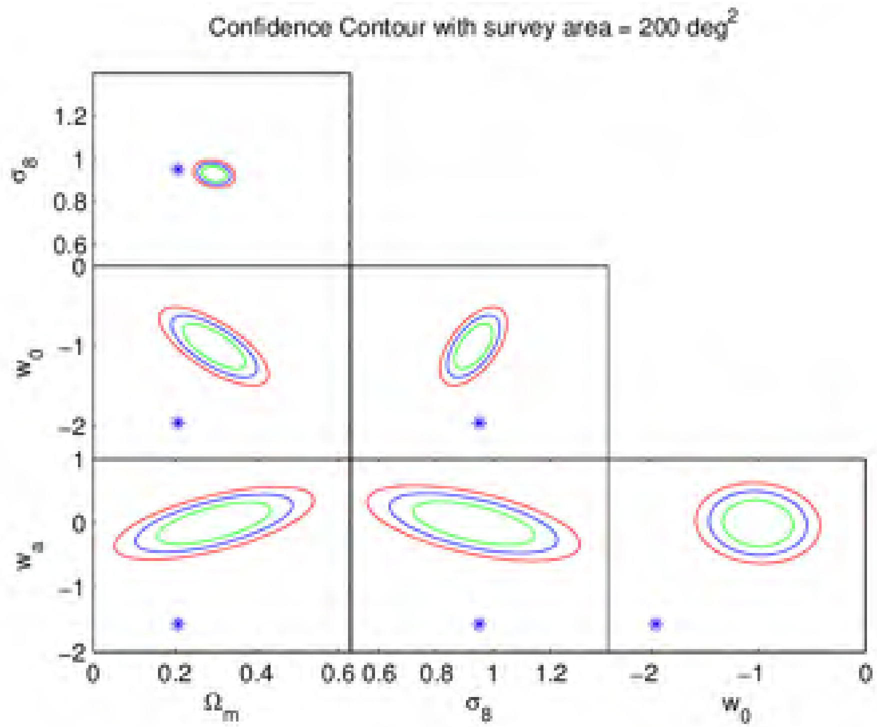

Zhang et al. 2012

Discussion

Noise effects can be modeled properly so that peak statistics directly from WL maps can potentially be used in cosmological studies

Other systematics: Projection effects (important for low peaks)

Baryonic effects on halo density profiles

** Effects of reconstruction method on WL peak statistics (Liu et al.)

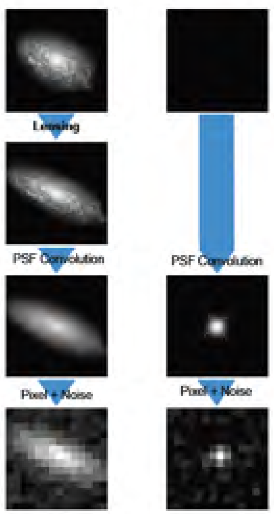

$$Q_{ij} = \frac{\int d^2\theta \, q_I[I(\boldsymbol{\theta})](\theta_i - \bar{\theta}_i)(\theta_j - \bar{\theta}_j)}{\int d^2\theta \, q_I[I(\boldsymbol{\theta})]}, \quad i, j \in \{1, 2\}$$

$$\varepsilon \equiv \frac{Q_{11} - Q_{22} + 2\mathrm{i}Q_{12}}{Q_{11} + Q_{22} + 2(Q_{11}Q_{22} - Q_{12}^2)^{1/2}}$$

$$< \varepsilon > \approx < g >, \; g = \frac{\gamma}{1 - \kappa}$$

$$\epsilon(\epsilon_s, z) = \begin{cases} \dfrac{\epsilon_s - g(z)}{1 - g^*(z)\,\epsilon_s} & \text{for} \quad |g(z)| \leq 1 \\ \dfrac{1 - g(z)\,\epsilon_s^*}{\epsilon_s^* - g^*(z)} & \text{for} \quad |g(z)| > 1 \end{cases}$$

Convergence reconstruction from shear measurements

$$<\varepsilon>\approx<g>,\ g=\frac{\gamma}{1-\kappa} \qquad \kappa(\boldsymbol{\theta})-\kappa_0=\frac{1}{\pi}\int_{\mathbb{R}^2}\mathrm{d}^2\theta'\,[1-\kappa(\boldsymbol{\theta}')]\,\Re[\mathscr{D}^*(\boldsymbol{\theta}-\boldsymbol{\theta}')\,\langle\varepsilon\rangle(\boldsymbol{\theta}')]$$

To assure the fast convergence of the iteration, we need to apply a smoothing first to get $<\varepsilon>\approx<g>$, and from that to obtain κ field.

Because $<g>=<\dfrac{\gamma}{1-\kappa}>\neq\dfrac{<\gamma>}{1-<\kappa>}$, the reconstructed κ field is

not the same as the smoothed κ field $<\kappa>$ that our model is based on.

→ bias when comparing observational results with models for LSST-like surveys.

However, the effects can be analyzed and potentially be correctable.

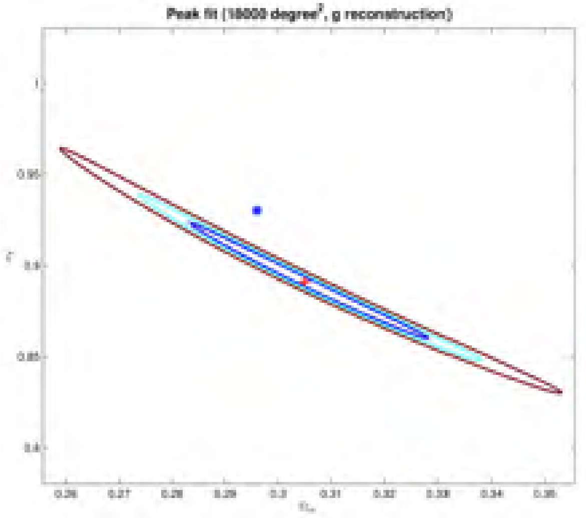

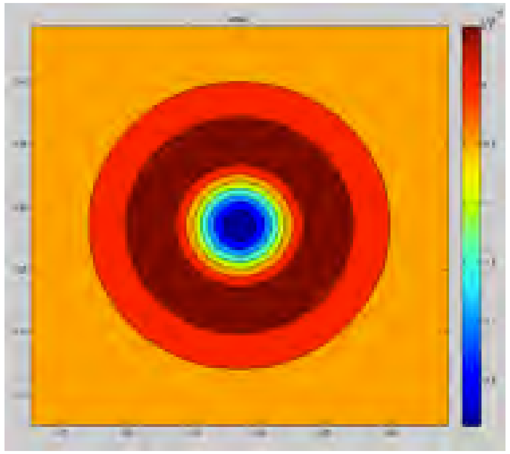

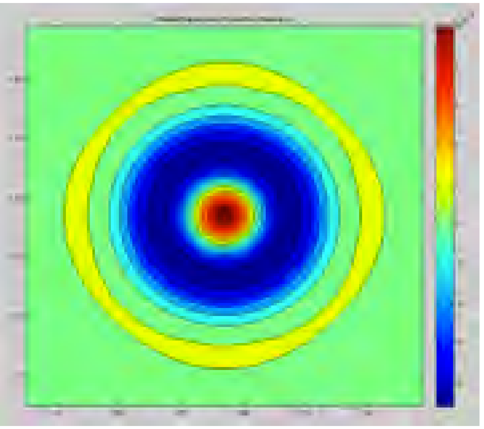

** Mask effects on WL peak statistics (Liu et al.)

The removal of bad data are inevitable in weak lensing observational analyses. The mask effects can be significant on peak statistics.

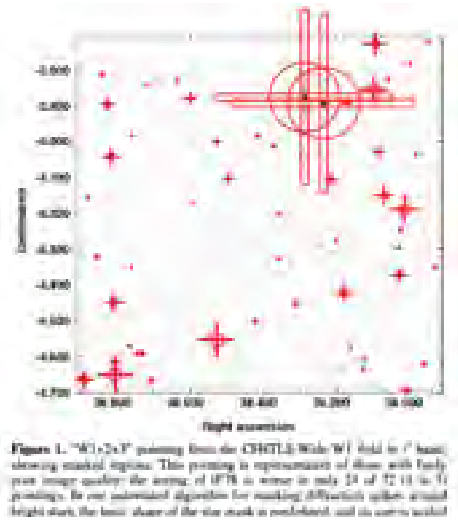

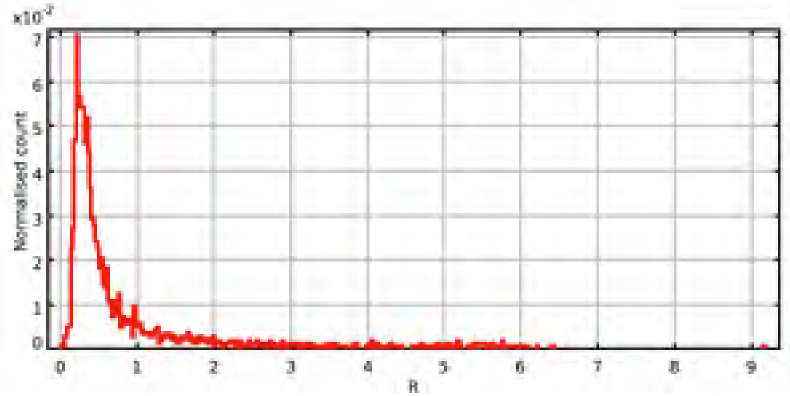

We are carrying out detailed analyses with numerical simulations.

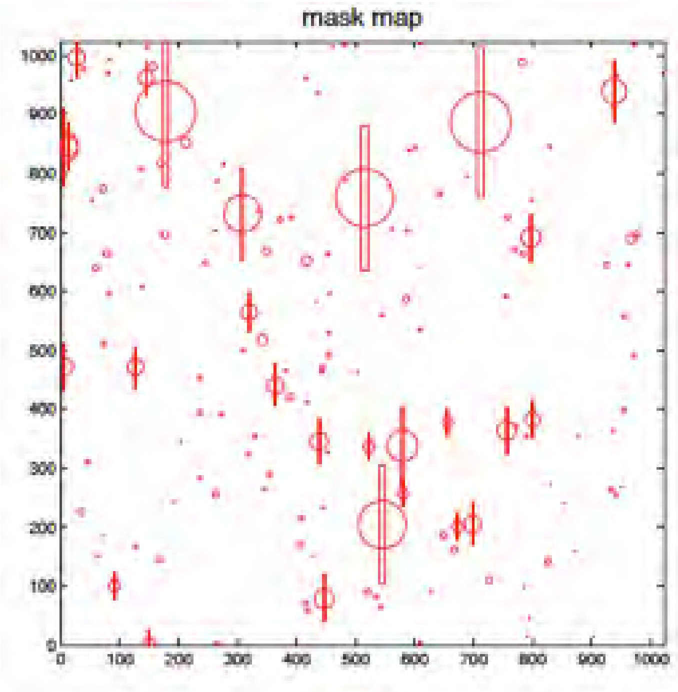

Mask effects can affect both the position and height of the peaks close to masked regions → the number of high peaks tend to be increased → can affect the inferred cosmological parameters significantly

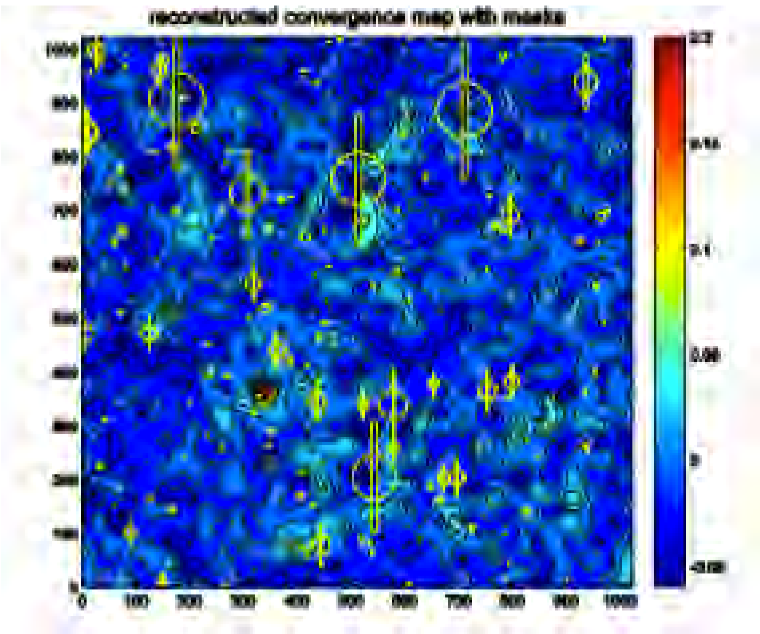

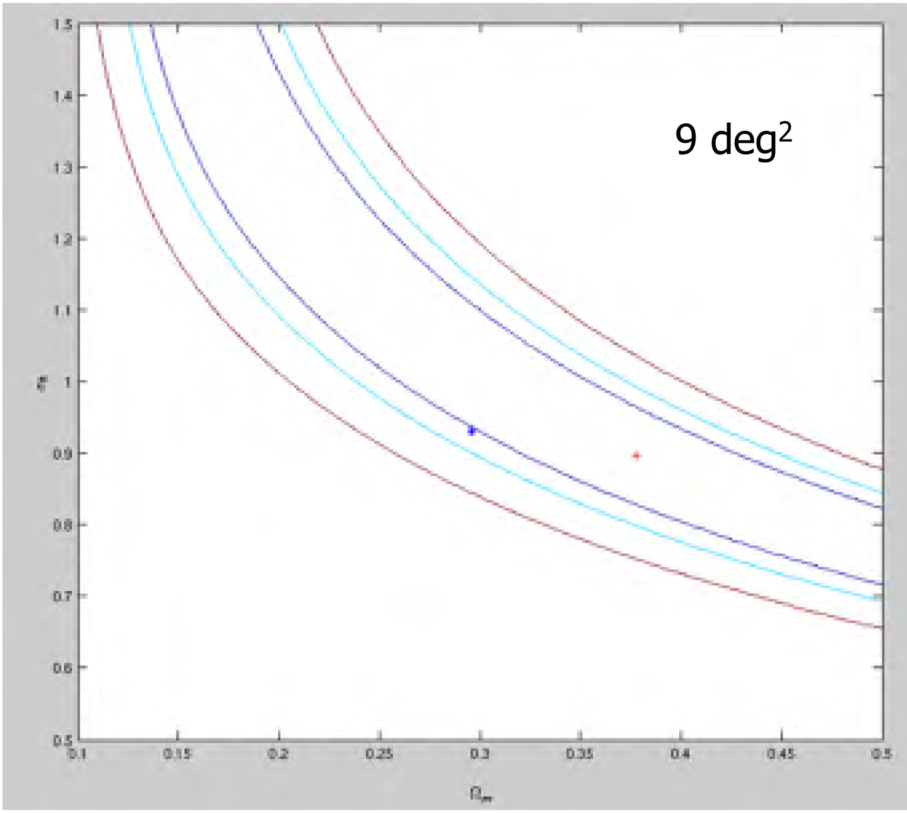

* How to handle the mask effects?

If large biases on cosmological parameters are introduced due to mask effects, one may consider to remove the large mask regions from peak counting. But the statistical errors are increased by doing so. Quantitative analyses are needed

* Develop models to correct mask effects, reconstruction bias

* Projection effects (including lower peaks in the analyses)

Future WL observations can detect large number of high peaks. With thorough understanding of different systematic effects, WL peak statistics can become a powerful probe in precision cosmological studies.

Thank you